Initial Development of Supercontinuum in Fibers with Anomalous Dispersion Pumped by Nanosecond-Long Pulses

Article *in* Optics Express · March 2008

DOI: 10.1364/OE.16.002636 · Source: PubMed

5 authors, including:

Nikolai Korneev
Instituto Nacional de Astrofísica, Óptica y Elect…
100 PUBLICATIONS **888** CITATIONS
SEE PROFILE

E. A. Kuzin
Instituto Nacional de Astrofísica, Óptica y Elect…
232 PUBLICATIONS **1,181** CITATIONS
SEE PROFILE

Baldemar Ibarra-Escamilla
Instituto Nacional de Astrofísica, Óptica y Elect…
223 PUBLICATIONS **1,018** CITATIONS
SEE PROFILE

Miguel Bello-Jiménez
Universidad Autónoma de San Luis Potosí
49 PUBLICATIONS **145** CITATIONS
SEE PROFILE

Initial development of supercontinuum in fibers with anomalous dispersion pumped by nanosecond - long pulses

N. Korneev, E. A. Kuzin, B. Ibarra-Escamilla, M. Bello-Jiménez A. Flores-Rosas

Instituto Nacional de Astrofísica, Optica y Electronica, Luis Enrique Erro No. 1, Departamento de Optica, Puebla Pue 72000, Mexico

korneev@inaoep.mx

Abstract: We propose and compare with experimental data a two-stage model of supercontinuum formation in a fiber for nanosecond-long pulse with intensities in 10W range. As a result of the first stage, the sea of solitons is formed. The second stage is spectrum modification because of Raman interaction.

OCIS codes: (190.4370) Nonlinear optics, fibers; (060.5530) Pulse propagation and temporal solitons.

References and links

1. J. K. Ranka, R. S. Windeler, and A. J. Stentz, "Visible continuum generation in air/silica microstructure optical fibers with anomalous dispersion at 800 nm," Opt. Lett. **25**, 25-27 (2000).
2. A. B. Fedotov, A. M. Zheltikov, A. A. Ivanov, M. V. Alfimov, D. Chorvat, Jr. Chorvat, V. I. Beloglazov, and D. Von Der Linde, "Supercontinuum-generating holey fibers as new broadband sources for spectroscopic applications," Laser Phys. **10**, 723-726 (2000).
3. T. A. Birks, W. J. Wadsworth, and P. St. J. Russell, "Supercontinuum generation in tapered fibers," Opt. Lett. **25**, 1415-1417 (2000).
4. A. B. Fedotov, A. M. Zheltikov, A. A. Ivanov, M. V. Alfimov, D. Chorvat, Jr. D. Chorvat, V. I. Beloglazov, and D. Von Der Linde, "Supercontinuum-generating holey fibers as new broadband sources for spectroscopic applications," Laser Phys. **10**, 723-726 (2000).
5. J. M. Dudley, L. Provino, N. Grossard, H. Mailotte, R. S.Windeler, B. J. Eggleton, and S. Coen, "Supercontinuum generation in air-silica microstructure fibers with nanosecond and femtosecond pulse pumping," J. Opt. Soc. Am. B **19,** 765-771 (2002).
6. B. R. Washburn, S. E. Ralph, and R. S. Windeler, "Ultrashort pulse propagation in air-silica microstructure fiber," Opt. Express **10**, 575-580 (2002).
7. F. Lu, Y. Deng, and W. H. Knox, "Generation of broadband femtosecond visible pulses in dispersion-micromanaged holey fibers," Opt. Lett. **30**, 1566-1568 (2005).
8. A. Ortigosa-Blanch, J. C. Knight, and P. St. J. Russell, "Pulse breaking and supercontinuum generation with 200-fs pump pulses in photonic crystal fibers," J. Opt. Soc. Am. B **19**, 2567–2572 (2002).
9. K. M. Hilligsøe, H. N. Paulsen, J. Thøgersen, S. R. Keiding, and J. J. Larsen, "Initial steps of supercontinuum generation in photonic crystal fibers," J. Opt. Soc. Am. B **20**, 1887-1893 (2003).
10. K. Mori, H. Takara, and S. Kawanichi, "Analysis and design of supercontinuum pulse generation in a single-mode optical fiber," J. Opt. Soc. Am. B **18**, 1780-1792 (2001).
11. S. Coen, A. H. L. Chau, R. Leonhardt, J. D. Harvey, J. C. Knight, W. J. Wadsworth, and P. St. J. Russel, "White light supercontinuum generation with 60-ps pump pulses in a photonic crystal fiber," Opt. Lett. **26**, 1356-1358 (2001).
12. L. Provino, J. M. Dudley, H. Maillotte, N. Grossard, R. S. Windeler, and B. J. Eggleton, "Compact broadband continuum source based on a microchip laser pumped microstructure fiber," Electron. Lett. **37**, 558-560 (2001).
13. A. A. Fotiadi, P. Mégret, "Self-Q-switched Er-Brillouin fiber source with extra-cavity generation of a Raman supercontinuum in a dispersion-shifted fiber," Opt. Lett. **31**, 1621-1623 (2006).
14. V. Avdokhin, S. V. Popov, and J. R. Taylor, "Continuous-wave, high-power, Raman continuum generation in holey fibers," Opt. Lett. **28**, 1353-1355 (2003).
15. C. Travers, R. E. Kennedy, S. V. Popov, J. R. Taylor, H. Sabert, and B. Mangan, "Extended continuous-wave supercontinuum generation in a low-water-loss holey fiber," Opt. Lett. **30**, 1938-1940 (2005).

#92272 - $15.00 USD Received 30 Jan 2008; accepted 4 Feb 2008; published 12 Feb 2008

16. A. K. Abeeluck, C. Headley, and C. G. Jørgensten, "High-power supercontinuum generation in highly nonlinear, dispersion-shifted fibers by use of a continuous-wave Raman fiber laser," Opt. Lett. **29**, 2163-2165 (2004).
17. W. Zhang, Y. Wang, J. Peng, and X. Liu, "Broadband high power continuous wave fiber Raman source and its applications," Opt. Commun. **231**, 371 – 374 (2004).
18. A. Mussot, E. Lantz, H. Mailotte, T. Sylvestre, C. Finot, and S. Pitois, "Spectral broadening of a partially coherent CW laser beam in single mode optical fibers," Opt. Express **12,** 2838-2843 (2004).
19. S. Martin-Lopez, A. Carrasco-Sans, P. Corderera, L. Abrardi, M. L. Hernanz, and M. Gonzalez-Herraez, "Experimental investigation of the effect of pump incoherence on nonlinear pump spectral broadening and continuous-wave supercontinuum generation," Opt. Lett. **31**, 3477–3479 (2006).
20. A. Podlipensky, P. Szarniak, N. Y. Joly, C. G. Poulton, and P. St. J. Russel, "Bound soliton pairs in photonic cristal fiber," Opt. Express **15**, 1653–1662 (2007).
21. M. Dudley, and S. Coen, "Numerical simulation and coherence properties of supercontinuum generation in photonic crystal and tapered optical fibers," IEEE J. Sel. Top. Quantum Electron. **8**, 651–659 (2002).
22. V. E. Zakharov and A. B. Shabat, "Exact theory of two-dimensional self-focusing and one-dimensional self-modulation of waves in nonlinear media," Sov. Phys. JETP **61**, 62-69 (1972).
23. A. Peleg, "Log-normal distribution of pulse amplitudes due to Raman cross talk in wavelength division multiplexing soliton transmission," Opt. Lett. **29**, 1980-1982 (2004).
24. B. A. Malomed, "Soliton-collision problem in the nonlinear Schrödinger equation with a nonlinear damping term," Phys. Rev. A **44**, 1412-1414 (1991).
25. G. P. Agrawal, *Nonlinear fiber optics*, (Optics and Photonics, 3rd ed., Ac. Press, San Diego, 2001).
26. S. Dyachenko, A. C. Newell, A. Pushkarev, V. E. Zakharov, "Optical turbulence: weak turbulence, condensates and collapsing filaments in the nonlinear Schrodinger equation" , Physica D **57**, 96-160 (1992).
27. E. A. Kuzin, S. Mendoza-Vasquez, J. Gutierrez-Gutierrez, B. Ibarra-Escamilla, J. W. Haus, and R. Rojas-Laguna, " Intra-pulse Raman frequency shift versus conventional Stokes generation of diode laser pulses in optical fibers," Opt. Express **13**, 3388-3396 (2005).

1. Introduction

The generation of supercontinuum (SC) in fibers obtained great attention after the demonstration of very broad SC in Photonic Crystal Fibers (PCF) [1,2] and tapered fibers [3]. Ultrasort fs-scale pulses are most commonly used for SC [4-9], however the SC generation was obtained also for ps pulses [10,11], ns pulses, [5,12,13] and even for cw pumping. For cw experiments different kinds of fibers were used: PCF [14,15], highly nonlinear fibers [16-18], and standard fibers [19]. Whereas the high peak power of ultrashort pulses is beneficial in SC generation in short fibers, relatively long (ns-scale) pulses and cw pumping are also discussed as an efficient and practical approach of the broadband signal generation. Various nonlinear processes are responsible for SC generation. For ultrashort pulses the Self Phase Modulation (SPM) play important role, the pulse breakup and intrapulse Raman scattering were also observed [1]. Numerical and experimental investigations have shown that both intrapulse Raman scattering and anti-Stokes generation occur early in fiber propagation [6]. It was found that the formation of the anti-Stokes component was not due to partially degenerate Four Wave Mixing (FWM). A detailed experimental study [8] of the behavior of 200-fs pulses in PCF has shown that Raman scattering leads to the breakup of higher-order soliton which is accompanied by the generation of radiation at shorter wavelengths. Also the bound soliton pairs in PCF were observed [20]. The cascaded stimulated Raman scattering (SRS) followed by the parametric FWM was reported in the experiment with 0.8-ns pulse [5]. For cw modulation instability (MI) was observed to seed spectral broadening and the interplay between MI and SRS was shown to play an important role in SC development [16,18]. The complexity of the detailed explanation of the SC relies on the fact that the interplay between the involved nonlinear processes is very sensitive to experimental conditions. Theoretical investigations of the SC generation are commonly carried out using the numerical solution of the nonlinear Schrodinger equation (NLSE) [6,21] and become prohibitively long for ns pulses. It is also important to note that it is difficult to get the physical insight in the process from numerical calculations.

#92272 - $15.00 USD Received 30 Jan 2008; accepted 4 Feb 2008; published 12 Feb 2008

We discuss approximations which permit to estimate spectrum widening in fibers with relatively long (1-100 ns range) and not very strong (typically, 5-50 W) input light pulses. Our approximation consists of two characteristic stages. The first stage is initial one when the pulse breaks into solitons mainly because of positive Kerr nonlinearity and anomalous dispersion. The power distribution of such solitons can be calculated with statistics of a long pulse breaking obtained in a well-known work of Zakharov and Shabat [22]. The next stage is interaction of solitons resulting from soliton collisions. Such collisions in a presence of Raman term lead to the amplification of more red-shifted soliton, and red shift in frequency of both solitons [23,24]. We consider this process in a framework of statistical model which takes into account interactions of different parts of the spectrum. The pulse is spread as a result of dispersion into the organized stream of solitons and background. The solitons, which are close spatially also have close frequencies. After this, the spectrum widening is caused mostly by the soliton self- frequency shift and it is drastically diminished in comparison with the second stage. We have measured the initial stage of the spectrum broadening in the fiber with anomalous dispersion pumped by 3-ns pulses. The experimental results suggest that this model gives a reasonable approximation for the spectra. Our results show, that the pulse width at nanosecond scale plays an important role in a spectrum widening, thus both small pulse width and cw simulations give only a part of total picture.

2. Theory

We consider the equation which describes pulse propagation in a fiber [25]:

$$\partial_z A = -i\frac{\beta_2}{2}\partial_t^2 A + i\gamma|A|^2 A - i\gamma T_R\left(\partial_t|A|^2\right)A \tag{1}$$

were A is signal amplitude, z is the propagation length, t is time, β_2 is second-order dispersion, γ is a nonlinear coefficient, and T_R is the characteristic time for Raman effect. We analyze the equation in two stages. Initially, the pulse is smooth, its spectrum is narrow, and at the first stage the Raman term in a right-hand side of Eq. (1) is negligible because it is proportional to a derivative of intensity. By neglecting this term, we obtain the Nonlinear Schrödinger Equation (NLSE). For the second stage we include the Raman term.

For NLSE it is known, that wide smooth pulses breakup practically completely into a big number of solitons (so called “sea of solitons”). Statistics of this breakup was found in [22], and it is based on the approximate semiclassical solution of associated scattering problem. The parameters of solitons which are formed upon propagation from a given initial pulse are found by finding isolated eigenvalues of Zakharov-Shabat scattering problem. The imaginary parts of these eigenvalues give soliton amplitudes, and their real parts correspond to soliton momenta. If the initial pulse is long and smooth, the eigenvalues are close to the imaginary axis, thus the solitons do not separate well under propagation.

We discuss here the simplest case of a long nearly rectangular pulse. Denoting pulse amplitude as, A_0 and its length as T, we have for the amplitude A_n of n-th soliton:

$$A_n = \frac{\rho_n\sqrt{|k|}}{2\cosh\left(k\rho_n(t-t_n)/2\right)}. \tag{2}$$

The parameter ρ is distributed approximately as

$$\rho_n = 4\sqrt{\frac{A_0^2}{|k|} - \frac{n^2\pi^2}{|k|^2T^2}} \tag{3}$$

where $k = \gamma/\beta_2$ and t_n are initial soliton positions. We do not consider the initial phases. Velocities of solitons are close to zero because real parts of scattering problem eigenfunctions

#92272 - $15.00 USD Received 30 Jan 2008; accepted 4 Feb 2008; published 12 Feb 2008

are close to zero. The total number of solitons is given by $N = |k|^{1/2} A_0 T \pi^{-1}$, and it is proportional to the pulse length, and the square root of intensity. The spectrum of the soliton set given by Eqs. (2) and (3) can be found by integration in a limit of a big soliton number and long distances between solitons. The result of the integration is presented in Fig. 1 by red line. The scaled frequency is used for which the maximal MI gain $\omega_0 = \sqrt{2|k|} A_0$ is equal to $\pi/(2\sqrt{2}) = 1.11$. The intensity was scaled to the maximum equal to one. The FWHM of the spectrum is equal to $1.2\omega_0$. The biggest soliton which is formed has peak intensity four times bigger, than the intensity of initial pulse, and the distribution given by the Eq. (2) demonstrates that small solitons are less frequent, than big ones. The form of the spectrum in the scaled coordinates does not depend on the pulse power, fiber dispersion, and fiber nonlinearity because all these parameters are included into the scaled frequency.

The solitons at formation have small velocities, thus initially they do not separate well by propagation, and remain inside the initial pulse. Thus, there is quite strong interaction between individual solitons, which leads to the spectrum modification. We compared the spectrum calculated from the statistical model of independent solitons with direct numerical simulations of Eq. (1), shown by points in the Fig. 1. For numerics we have taken the initial condition as constant amplitude with a small addition of white noise in a limited frequency band. The equations were solved with a split-step method [25], which corresponds to periodic in time solution. The solution was run for a long enough distance, and average values for spectra with different realizations of initial noise were taken. The simulation demonstrates that the spectrum in comparison to that one of independent solitons is modified mainly in a low-frequency region, where narrow peak appears. There is also some spectrum modification around the MI band. For the second stage of the spectrum widening, the form of high-frequency tail is important, and for it the simulation and approximation of independent solitons agree quite well.

From the associated eigenvalue problem it is possible to determine the number and parameters of solitons which emerge, but the scattering problem solution does not say which propagation distance is necessary for soliton formation. This distance has to be of an order of some MI lengths, and depends weakly on initial noise level.

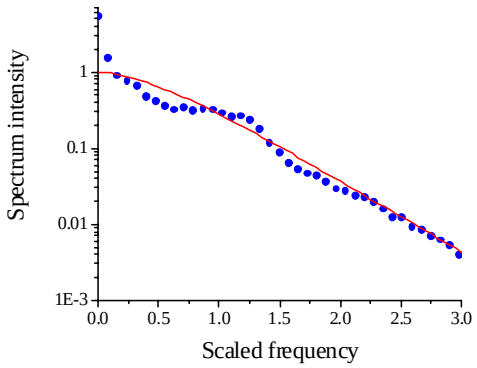

Fig. 1. The spectrum of a sum of solitons according to Zakharov-Shabat statistics of soliton sea (red line), and the result of numerical simulation for breakup of a long pulse with initially small white noise (blue circles). Approximately 18 solitons are formed. It is seen, that the high-frequency tail is well described by a spectrum resulting from the superposition of independent solitons.

#92272 - $15.00 USD Received 30 Jan 2008; accepted 4 Feb 2008; published 12 Feb 2008

At the second stage the Raman effect is included. When the first stage is finished, the soliton sea formation is complete. Now, there is a collection of individual solitons, and the spectrum is enriched to width equal approximately to the wavelength difference between the MI maxima. The spectrum has exponentially decaying tails. Individual solitons in medium with Raman nonlinearity have self-frequency shift which is determined by Raman amplification of smaller frequencies inside an individual soliton. The experimental data and numerics demonstrate that such shift can be important for intermediate stage between the formation of the soliton sea and the second phase. However, for solitons with different central frequencies, the interactions between different solitons are more important. In fact, the frequency differences between solitons are bigger, than inside individual ones, thus the Raman term due to interference is bigger than the term resulting from individual soliton shape. With Raman nonlinearity present, the solitons do not just pass one through another. After each collision, the soliton with a bigger red shift becomes bigger, and both solitons gain additional red shift [23,24]. Apart from this, after each collision, some part of the total energy is lost to a non-soliton background.

Instead of soliton-soliton interaction we consider for a second stage a simple model derived directly from the Eq. (1). To obtain it, we act similar to the approach of so called weak optical turbulence [26]. First, we express the wave function in terms of its Fourier spectrum.

$$A(t,z)=\sum_{\omega}A(\omega,z)\exp(i\omega t). \tag{4}$$

With Eqs. (4) and (1) we get for the evolution of the intensity at a given spectral component the expression (we omit the explicit z-dependence of spectrum):

$$\begin{aligned}&\partial_z\left(A(\omega)A^*(\omega)\right)=\\&i\gamma\sum_{\omega1+\omega2=\omega3+\omega}A(\omega_1)A(\omega_2)A^*(\omega_3)A^*(\omega)\left(1-iT_R(\omega_1-\omega_3)\right)-c.c.\end{aligned} \tag{5}$$

We note, that if spectral components at different frequencies are not correlated, then phases of products at the right-hand side are generally random, and the most important contribution is obtained for a degenerate interaction, when $\omega_1 = \omega$, or $\omega_2 = \omega$. For this to be true, the difference between frequencies (i.e. the total spectrum width) has to be bigger than the spectral width of participating solitons. Such approximation can hold for a developed Raman stage. If only degenerate interactions are taken into account, the Eq. (5) is written (we change a sum into an integral) as

$$\frac{\partial_z\left|A(\omega,z)\right|^2}{\left|A(\omega,z)\right|^2}=2\gamma T_R\int d\omega'(\omega-\omega')\left|A(\omega,z)\right|^2. \tag{6}$$

Where $\left|A(\omega,z)\right|^2$ is the intensity of the spectrum component. Note, that in this approximation the Kerr nonlinearity does not result in a spectrum spreading; this is true if characteristic frequency differences are bigger, than the modulation instability limit frequency. The Eq. (6) conserves the total power $E=\int d\omega\left|A(\omega)\right|^2$.

The Eq. (6) with an initial condition $\left|A(\omega,0)\right|^2=\left|A_0(\omega)\right|^2$ has a solution

$$\left|A(\omega,z)\right|^2=\frac{\left|A_0(\omega)\right|^2 E\exp\left(2\gamma T_R E\omega z\right)}{\int d\omega'\left|A_0(\omega')\right|^2\exp\left(2\gamma T_R E\omega' z\right)} \tag{7}$$

#92272 - $15.00 USD Received 30 Jan 2008; accepted 4 Feb 2008; published 12 Feb 2008

For Eq. (7) to hold, it is necessary for the intensity spectrum to diminish quite rapidly with frequency, and for big z the formal solution of Eq. (7) will finally transfer the spectrum to a low-frequency region. This is related to the fact that the Raman amplification is most important for big frequency difference. To avoid this, we were limiting initial spectrum width to 100 nm, which is approximately the maximum of Raman amplification spectra.

For a short pulse, after the spectrum is enriched by Raman interaction, the red spectral components will be separated at one end of the pulse, and blue ones at another. This will spread the pulse, diminish a local spectral range, and diminish further frequency spreading of a spectrum. We model this situation by separating initial pulse into sections, which are much longer than individual solitons, but much shorter than a total pulse length. In each section with number *P* we have its own spectral distribution $I_P(\omega, z)$. Along propagation, spectral components travel with different frequencies, determined by the second-order dispersion, thus we modify after each step *dz*, the $I_P(\omega, z)$ according to the values of $I_{P\pm1}(\omega, z)$ and the frequency value. The net result is the spreading of initial pulse, and diminishing of spectrum enrichment when spectral components are separated along the pulse. At the final of the second stage one can expect the formation of strongly red-shifted solitons with intensities higher than the four-time initial power characteristic of the first stage.

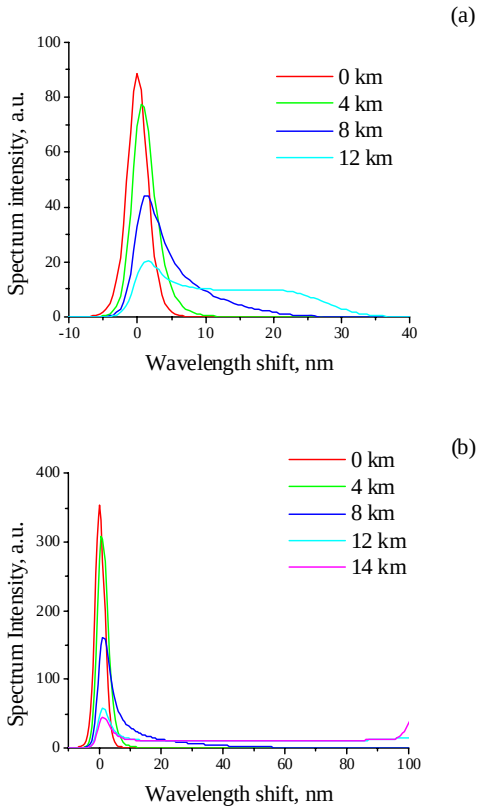

Fig. 2. The developing of the spectra with fiber length calculated from Eq. (7); (a) for 3 ns pulses and (b) for 12 ns pulses. Fiber parameters are close to those used in experiment.

#92272 - $15.00 USD Received 30 Jan 2008; accepted 4 Feb 2008; published 12 Feb 2008

Figure 2 shows the typical solution spectra for 3-ns pulses, Fig. 2(a) and 12-ns pulses Fig. 2(b). The spectrum for $L = 0$ represents the initial condition. The pulse power was 10 W. We have taken as an initial condition the spectrum of a single soliton with an adequate width, but similar results are obtained for other realistic initial distributions. The spectra were scaled to have the area under curves proportional to the pulse energy. Both figures show similar behavior of the spectrum. First the spectrum moves to the longer wavelength, then the flat part appears. The flat part spreads to longer wavelength while the fiber length increases. However for the 12-ns pulse the flat part is longer than that for the 3-ns pulse. For long pulses, Raman amplification for long wavelength components becomes very strong, that finally transfers all energy of pump into a Stokes component with wavelength shift determined by the maximum of the Raman amplification. In the approximation that the Eqs. (6) and (7) give this means that after some propagation length the spectrum moves to strongly red-shifted region. Fig. 2(b) shows that the growth of the spectrum intensity for 14-km fiber begins at 100-nm of the wavelength shift. However the Eq. (1) supposes the linear growth of the Raman amplification with the wavelength shift that it is not valid for long wavelength shift and one has to use the equation in more general form to investigate this part of spectrum.

Finally, when solitons are well separated, the only effect leading to spectrum enrichment can be self-frequency shift of individual solitons. This is expected to be much slower than the spectrum widening at the second stage. The model does not predict, how much of the initial intensity will remain in a form of solitons. (In fact, the soliton-soliton collisions with Raman perturbation produce non-soliton components as well.)

3. Experimental results

The experiments were made using the SMF-28 fiber with dispersion D equal to 20 ps/nm-km and the core area equal to 81 μm^2. Pulses were generated by directly modulated DFB laser and amplified by the two-stage EDFA. The experimental setup is similar to that described in [27] were the broad band spectrum generation by 3 ns and 30 ns pulses was investigated. In particular it was found that for 3 ns pulse the flat spectrum was generated. The spectrum did not show any maximum at the wavelength shift of the Raman amplification maximum. But for the 30-ns pulses the Stokes generation at 1660 nm was observed. That corroborates with the results shown in the Fig. 2. In this paper we focused on the initial stage of the spectrum formation at respectively low power. The second stage of the model supposes that the most part of solitons are still within the time slot defined by the initial pump pulse. For this the delay between the spectral components has to be less than the pulse duration. The fiber length respectively has not to be too long.

Figure 3 shows spectra measured at the end of the fibers in the length range between 100 m and 8 km; 3-ns pulses were used.

#92272 - $15.00 USD Received 30 Jan 2008; accepted 4 Feb 2008; published 12 Feb 2008

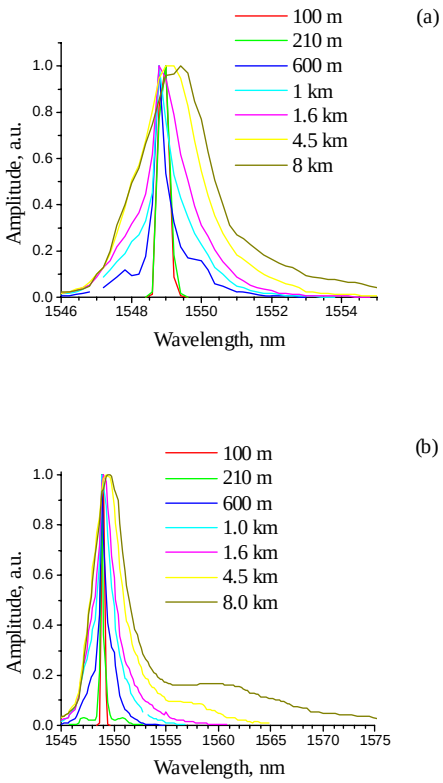

Fig. 3. Comparative spectra at two fixed powers for series of length between 100 m and 8.0 km; (a) the pulse power is 6 W, (b) the pulse power is 10 W.

Figure 3(a) shows results for 6-W pulses. For 100-m fiber and for 210-m fiber no nonlinear broadening of the spectrum is observed. The line width in this case is defined by the monochromator resolution. For 600-m fiber the MI peaks appear. The wavelength difference between the peaks is equal to 2.2 nm. Analytically calculated shift of the MI amplification maximum [25] is equal to 1.08 nm for the fiber with nonlinearity $\gamma = 1.59 W^{-1} km^{-1}$ and dispersion $|\beta_2| = 25\ ps^2 / km$. For the 1.6-km fiber the spectrum becomes similar to that shown in the Fig. 1 with FWHM equal to 1.14 nm. If we consider that the spectrum width is defined mostly by the highest solitons, we can estimate that the highest solitons have power about 10 W or two times higher than the input pulse. For the 4.5 km the spectrum is still very close to symmetrical one with FWHM equal 2.07 nm that gives the power of the highest soliton equal to 32 W or 5 times higher than the input power. These values are close to the theoretical results showing that the biggest soliton has four times higher peak intensity than the input pulse. Those are only rough estimation taking into account the quadratic dependence of the soliton power on its width and the fact that the resolution of the monocromator equaled to 0.4 nm is not sufficiently good. The 8-km fiber demonstrates a well defined red shift of the spectrum. For 10-W pulses the behavior is similar, see Fig. 3(b). The MI side lobes appear for the 210-m fiber with wavelength shift between them equal to 3.7 nm. FWHM width of the spectrum for the 1.6-km fiber is equal to 1.54 nm that gives the power of the biggest soliton equal to 58 W, i.e. approximately four times higher than the input power. For longer fiber lengths the red shift appears. It is interesting to note that if we take the soliton with power equal to 58 W and launch it to the fiber with loss equal 0.2 dB/km the calculated shift caused

#92272 - $15.00 USD Received 30 Jan 2008; accepted 4 Feb 2008; published 12 Feb 2008

by soliton self frequency shift is only 2.5 nm. However in experiment we see the spectral broadening for the 8-km fiber which is more than 25 nm. This strong red shift agrees with the theoretical consideration of the Raman shift at soliton-soliton collisions.

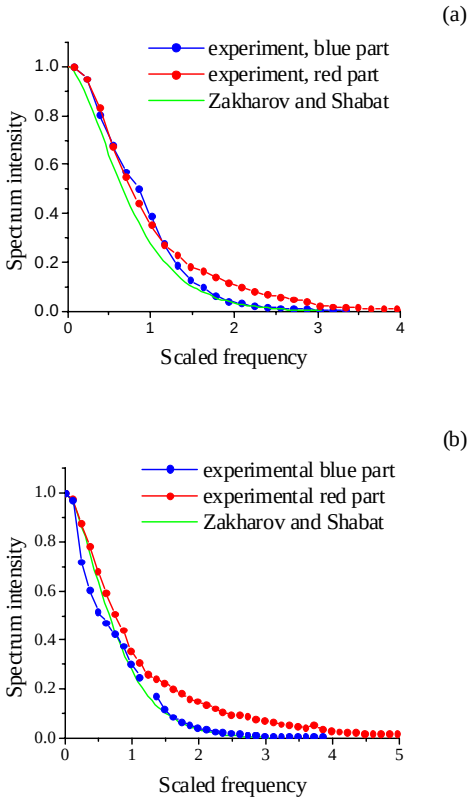

Fig. 4. Comparison between experimental and Zakharov and Shabat spectra; (a) 6-W pump and 4.5-km fiber; (b) 10-W pump and 1.6-km fiber.

Figure 4 shows the theoretical and experimental spectra depicted in the same scale to make the comparison between Zakharov and Shabat spectrum and experimentally measured spectrum. The experimental spectra are folded so the “blue” part and “red” part of the spectrum appear in the same quadrant. We did this to see asymmetry of the experimental spectrum. To make scaling of the experimental data we used experimentally measured shift of the MI maxima equal to 1.1 nm and 1.85 nm for 6 W and 10 W respectively. The experimental spectrum is very similar to the theoretical one for 6-W pump. For 10-W pump the asymmetry appears and the “red” shift can be seen.

The increase of the fiber length at 10-W power results in gradual growth of the “red” tail, however the central part of the spectra remains to be similar to the Zakharov and Shabat spectrum, see Fig. 5.

#92272 - $15.00 USD Received 30 Jan 2008; accepted 4 Feb 2008; published 12 Feb 2008

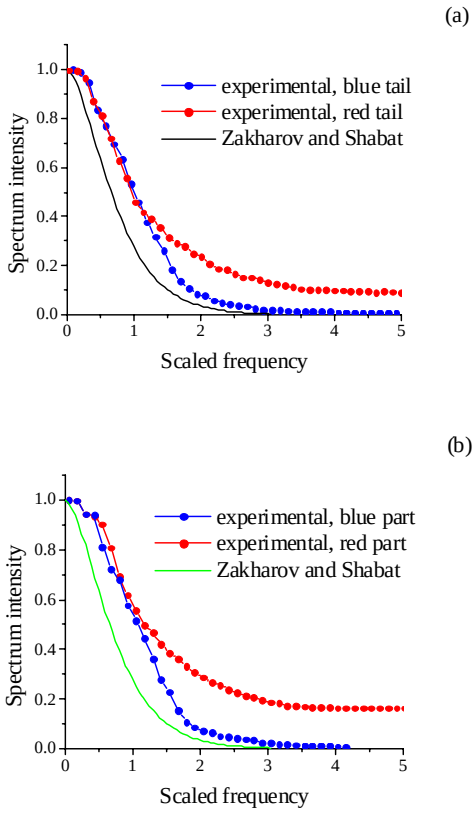

Fig. 5. The growth of the red tail with fiber length for 10-W pump pulses; (a) for the 4.5 km fiber and (b) for the 8-km fiber.

4. Conclusions

The presented two-stage model qualitatively well describes the experimentally observed spectrum behavior, giving good estimations of spectral shape and width upon propagation. Two stages are clearly observed in the experiment. At the first stage, the pulse breaks into solitons, with statistics described by a semiclassical approximation to Zakharov and Shabat scattering problem. At this stage the spectrum is symmetric and has a characteristic width of modulation instability band with exponentially decaying tails. At the second stage, the spectrum, enriched at the first stage, expands to the red region because of Raman amplification of red-shifted parts of a spectrum. The process can be alternatively regarded as collisions of solitons with different central frequencies with modification of their amplitudes and central frequencies. The form and width of resulting spectra are reasonably well described by the suggested model given by Eqs. (6) and (7). The advantage of presented model is its simplicity. Different of the direct numerical solution of Eq. (1), the model permits intuitive understanding of underlying processes. Both short-pulse simulations, and continuum wave simulations are not adequate for nanosecond pulses, and the pulse width in this range affects spectrum enrichment parameters.

Acknowledgments

This investigation was supported by the CONACYT project 47169.

#92272 - $15.00 USD Received 30 Jan 2008; accepted 4 Feb 2008; published 12 Feb 2008